Effects of Substrate Surface Functionality on Solution-Deposited Titania Films

Hillel Pizem and Chaim N. Sukenik

Department of Chemistry, Bar-Ilan University, Ramat-Gan, Israel

Uma Sampathkumaran,† Alan K. McIlwain, and Mark R. De Guire*

Department of Materials Science & Engineering, Case Western Reserve University, Cleveland, Ohio, 44106-3317

Received August 28, 2001. Revised Manuscript Received March 15, 2002

Liquid-phase deposition (LPD) from aqueous solution, under mild conditions of temperature (≤55 °C) and pH (2.88−3.88), can produce thin (0.1−1.0 μm), adherent titania (TiO_2) films. This paper reports a systematic study of LPD TiO_2 films on variously prepared silicon wafer substrates, including (to our knowledge for the first time with LPD) several types of sulfonated surfaces (including sulfonated self-assembled monolayers and sulfonated polyelectrolyte multilayers). The growth rate and crystallinity of these films could be controlled by careful manipulation of solution parameters and surface functionality of the substrate.

Introduction

Techniques for synthesizing inorganic oxide thin films from low-temperature liquid solutions have received increasing interest in recent years. Lower temperatures allow films to be deposited on substrates that might not be chemically or mechanically stable at high temperatures. Unlike vapor-phase processes, techniques that use liquids as the deposition medium do not rely on line-of-sight deposition, enabling nonplanar substrates to be coated. The equipment for liquid-based techniques is simple and much less costly than, for example, vacuum systems and gloveboxes. Finally, with aqueous solutions and readily available reagents, there is reduced reliance on expensive or sensitive organometallic precursors and the potential for reduced environmental impact, in comparison with many chemical routes. Niesen and De Guire have reviewed nonelectrochemical, non-hydrothermal aqueous routes to oxide thin films.[1]

Liquid-phase deposition (LPD) is an aqueous technique for deposition of oxide films that has been widely used for SiO_2[2] but is being studied increasingly as a route for films of other oxides such as titania[3−10] and others (reviewed in ref 1). It was first reported in a 1950 patent to Thomsen et al.[11] In the 1980s Kawahara and co-workers patented a related method for coating glass with TiO_2.[12,13] The distinguishing characteristic of LPD is the use of a solution of metal−fluoride complexes whose hydrolysis in water is modulated by adding boric acid (H_3BO_3) or aluminum metal. The fluoride ligand provides for a slower and more controllable hydrolysis, while the boric acid or the aluminum function as F^- scavengers.[14]

The role of solution chemistry in the deposition of films from aqueous solutions, whether by LPD or by other techniques, has been a dominant theme in the literature. The various methods that have been reported can be categorized based on characteristic approaches to maintaining the supersaturation of the solution so as to sustain the formation of the solid phase.[1] In all methods, small differences in pH, temperature, or solution composition can have large effects on the solution's supersaturation, significantly affecting the form and growth rate of the resulting films.

On the other hand, the role of the substrate in aqueous depositions of oxide films has been the subject of a smaller number of systematic studies.[15−19] One strategy that has been used to control the chemical nature of the substrate surface has been the use of

* To whom correspondence should be addressed at Department of Materials Science & Engineering, Case Western Reserve University, 10900 Euclid Avenue, Cleveland, OH 44106-7204. Tel.: 216-368-4221. Fax: 216-368-8932. E-mail: mrd2@po.cwru.edu.

† Present address: Optinetrics, Inc., 20410 Earl St., Torrance, CA 90503.

(1) Niesen, T. P.; DeGuire, M. R. *J. Electroceram.* **2001**, *6*, 169−207.

(2) Nagayama, H.; Honda, H.; Kawahara, H. *J. Electrochem. Soc.* **1988**, *135*, 2013−2016.

(3) Deki, S.; Aoi, Y.; Hiroi, O.; Kajinami, A. *Chem. Lett.* **1996**, 433−434.

(4) Deki, S.; Aoi, Y.; Yanagimoto, H.; Ishii, K.; Akamatsu, K.; Mitzuhata, M.; Kajinami, A. *J. Mater. Chem.* **1996**, *6*, 1879−1882.

(5) Deki, S.; Aoi, Y.; Asaoka, Y.; Kajinami, A.; Mizuhata, M. *J. Mater. Chem.* **1997**, *7*, 733−736.

(6) Shimizu, K.; Imai, H.; Hirashima, H.; Tsukuma, K. *Thin Solid Films* **1999**, *351*, 220−224.

(7) Koumoto, K.; Seo, S.; Sugiyama, T.; Seo, W. S. *Chem. Mater.* **1999**, *11*, 2305−2309.

(8) Imai, H.; Takei, Y.; Shimizu, K.; Matsuda, M.; Hirashima, H. *J. Mater. Chem.* **1999**, *9*, 2971−2972.

(9) Imai, H.; Matsuta, M.; Shimizu, K.; Hirashima, H.; Negishi, N. *J. Mater. Chem.* **2000**, *10*, 2005−2006.

(10) Yamabi, S.; Imai, H. *Chem. Lett.* **2001**, 220−221.

(11) Thomsen, S. M.; Nicoll, F. H. Radio Corporation of America, U.S.A., U.S. Patent 2,505,629, 1950.

(12) Kawahara, H.; Honda, H. Nippon Sheet Glass Co. Ltd.: Japan, 1984.

(13) Ino, J.; Hishinuma, A.; Nagayama, H.; Kawahara, H. Nippon Sheet Glass Co. Ltd., Japan, Japanese Patent 59141441A, 1989.

(14) Wamser, C. A. *J. Am. Chem. Soc.* **1951**, *73*, 409−412.

(15) Nagtegaal, M.; Stroeve, P.; Tremel, W. *Thin Solid Films* **1998**, *327−329*, 571−575.

10.1021/cm010776e CCC: $22.00
Published on Web 05/09/2002

organic self-assembled monolayers (SAMs). A SAM is a close-packed, highly ordered array of long-chain hydrocarbon molecules anchored to a solid substrate by strong covalent or ionic bonds.[20] The functional group on the SAM terminus remote from the anchoring functionality is responsible for the surface properties and can play a role in ceramic film deposition. Using this approach, compact, uniform, and adherent thin films of TiO_2,[7,19,21−28] SnO_2,[29,30] $V_2O_5 \cdot nH_2O$,[17,18] three different polymorphs of FeOOH,[15,16,31−33] and several other oxides (reviewed elsewhere[1]) have been deposited. While most of these studies have shown that the SAM promotes the formation of the oxide film, the specific role of the SAM remains a subject of study. Tarasevich, Rieke, and co-workers[32,33] attribute the effect to an enhancement in the heterogeneous nucleation of solid on the SAM surface, resulting from a decrease in the surface energy of the SAM relative to that of a bare substrate. Aizenberg et al.[34] observed highly specific and exclusive orientations of calcite crystals forming on variously functionalized SAMs. They attribute this to unique coincidences between functional group spacing and the spacing between carbonate groups in the selected planes of the crystal. In cases where nucleation occurs in the bulk solution (away from the substrate), Shin et al.[35] postulate that the SAM can increase the van der Waals and electrostatic attractions between the SAM and the existing solid particles, contributing to the formation of the film.

Another approach to modifying an inorganic surface is to use organic polyelectrolytes. This approach has been used to deposit nanostructured organic−inorganic composite films consisting of alternating layers of polyelectrolytes and TiO_2.[36,37] (See ref 38 for a review.)

The present work attempts to elucidate the role of the substrate during LPD of TiO_2 films by using silicon wafers with different types of surface treatments. Given their proven effect in other solution deposition processes,[21,29−33] variously sulfonated surfaces are a focus of this work.

While this paper focuses on the effects of the substrates, the structure and properties of the resulting film often depend on both the substrate and the solution. To illustrate this interdependence, the present work also explores effects of discrete differences in LPD solution parameters, using conditions similar to two published LPD routes for the deposition of TiO_2.[3,7] We find that small differences in pH, temperature, and solution composition can lead to dramatic differences in the film's crystallinity, adherence, and growth rate. Furthermore, the two routes used here exhibit entirely different deposition behavior toward bare silicon surfaces and toward sulfonate-bearing surfaces. These effects are explained in terms of the structure and surface charge of the substrates, differences in the degree of supersaturation of the solutions, and the structure of anatase (the form of TiO_2 observed in the present work when the film was not amorphous).

Experimental Section

Materials. "Prime grade" ⟨100⟩ p-type silicon wafers polished on one side were purchased from Silicon Sense Inc. All commercial reagents and solvents were purchased from Aldrich and used as received, unless otherwise specified. 1-Thioacetate-16-(trichlorosilyl)hexadecane was prepared as previously reported.[39] Water was deionized and distilled in an all-glass apparatus.

Equipment. UV ozone cleaning of substrates was done using a UVOCS Model 10-X10/OES/E. Solution pH was measured using a Metrohm model 691 pH meter. Wetting properties were assessed by water contact angle measurements using a Rame Hart Model 100 Contact Angle Goniometer. Optical microscopy (up to 1000×) was done using an Olympus Model BX-60 microscope equipped with a U-PO polarizer, a U-AN-360 analyzer, and a U-DICR Nomarsky lens. Pictures were taken with a Nikon CoolPix 990 digital camera. Scanning electron microscopy (SEM) was performed on a Philips XL-30 ESEM in the high-vacuum mode, typically at 15 keV. A Noran Vantage energy-dispersive X-ray system was used for elemental analysis and image analysis. Ellipsometry was done using a Woollam M-44 variable angle spectroscopic ellipsometer, using WVASE 32 software (version 3.154). Grazing incidence X-ray diffraction (XRD) analysis at 0.5° and 1° incidence was done on a SCINTAG XI Advanced Diffraction System composed of a 4.0-kW ultrastable generator, a 2-kW X-ray diffraction tube (Cu target), and a $\theta-\theta$ wide angle goniometer. The system is also equipped with a thin film grazing angle collimation attachment. Rutherford backscattering spectroscopy (RBS) was carried out using a NEC 5SDH ion beam accelerator and beam energy of 2 MeV. The energy of the elastically scattered alpha particles after impinging on the thin

(16) Nagtegaal, M.; Stroeve, P.; Ensling, J.; Gütlich, P.; Schurrer, M.; Voit, H.; Flath, J.; Käshammer, J.; Knoll, W.; Tremel, W. *Chem. Eur. J.* **1999**, *5*, 1331−1337.
(17) Niesen, T. P.; Wolff, J.; Bill, J.; DeGuire, M. R.; Aldinger, F. In *Organic−Inorganic Hybrid Materials II*; Klein, L. C., Francis, L. F., DeGuire, M. R., Mark, J. E., Eds.; Materials Research Society: Warrendale, PA, 1999; Vol. 576, pp 197−202.
(18) Niesen, T. P.; Wolff, J.; Bill, J.; Wagner, T.; Aldinger, F. In *Proceedings 9th CIMTEC−World Forum on New Materials, Symposium III − Surface Engineering*; Vincenzini, P., Ed.; Techna: Faenza, Italy, 1999; Vol. 20, pp 27−34.
(19) Niesen, T. P.; Bill, J.; Aldinger, F. *Chem. Mater.* **2001**, *13*, 1552−1559.
(20) Ulman, A. *Chem. Rev.* **1996**, *96*, 1533−1554.
(21) Shin, H.; Collins, R. J.; DeGuire, M. R.; Heuer, A. H.; Sukenik, C. N. *J. Mater. Res.* **1995**, *10*, 692−698.
(22) Huang, D.; Xiao, Z. D.; Gu, J. H.; Huang, N. P.; Yuan, C. W. *Thin Solid Films* **1997**, *305*, 110−115.
(23) Baskaran, S.; Song, L.; Liu, J.; Chen, Y. L.; Graff, G. L. *J. Am. Ceram. Soc.* **1998**, *81*, 401−408.
(24) Xiao, Z.; Gu, J.; Huang, D.; Lu, Z.; Wei, Y. *Appl. Surf. Sci.* **1998**, *125*, 85−92.
(25) Xiao, Z.; Su, L.; Gu, N.; Wei, Y. *Thin Solid Films* **1998**, *333*, 25−28.
(26) Xiao, Z.; Xu, M.; Gu, J.; Huang, D.; Lu, Z. *Mater. Chem. Phys.* **1998**, *52*, 170−174.
(27) Niesen, T. P.; DeGuire, M. R.; Bill, J.; Aldinger, F.; Rühle, M.; Fischer, A.; Jentoft, F. C.; Schlögl, R. *J. Mater. Res.* **1999**, *14*, 2464−2475.
(28) Masuda, Y.; Sugiyama, T.; Lin, H.; Seo, W. S.; Koumoto, K. *Thin Solid Films* **2001**, *382*, 153−157.
(29) Bunker, B. C.; Rieke, P. C.; Tarasevich, B. J.; Campbell, A. A.; Fryxell, G. E.; Graff, G. L.; Song, L.; Liu, J.; Virden, J. W.; McVay, G. L. *Science* **1994**, *264*, 48−55.
(30) Supothina, S.; DeGuire, M. R. *Thin Solid Films* **2000**, *371*, 1−9.
(31) Rieke, P. C.; Marsh, B. D.; Wood, L. L.; Tarasevich, B. J.; Liu, J.; Song, L.; Fryxell, G. E. *Langmuir* **1995**, *11*, 318−326.
(32) Tarasevich, B. J.; Rieke, P. C. *Chem. Mater.* **1996**, *8*, 292−300.
(33) Rieke, P. C.; Wiecek, R.; Marsh, B. D.; Wood, L. L.; Liu, J.; Song, L.; Fryxell, G. E.; Tarasevich, B. J. *Langmuir* **1996**, *12*, 4266−4271.
(34) Aizenberg, J.; Black, A. J.; Whitesides, G. M. *J. Am. Chem. Soc.* **1999**, *121*, 4500−4509.
(35) Shin, H.; Agarwal, M.; DeGuire, M. R.; Heuer, A. H. *Acta Mater.* **1998**, *46*, 801−815.
(36) Kotov, N. A.; Dekany, I.; Fendler, J. H. *J. Phys. Chem.* **1995**, *99*, 13065−13069.
(37) Liu, Y.; Wang, A.; Claus, R. *J. Phys. Chem. B* **1997**, *101*, 1385−1388.
(38) Fendler, J. H. *Chem. Mater.* **1996**, *8*, 1616.
(39) Collins, R. J.; Sukenik, C. N. *Langmuir* **1995**, *11*, 2322−2324.

Table 1. Liquid-Phase Deposition of TiO_2 for 22 h on Variously Cleaned/Modified Si Wafers

no.	substrate[a]	method[b]	film appearance[c]	thickness by RBS and [ellipsometry]	form
1a,b	**P,U**	2	patchy, nonadherent		
2	**P**	1	excellent uniformity, adherent (Figure 1b)	230 nm + 75 nm roughness [287 nm]	amorphous
3	**U**	1	uniform, adherent	[308 nm]	amorphous
4	**C**	1	uniform, adherent	[260 nm]	amorphous
5	**C_{16}TA**	1	no film		
6	**C_{16}TA**	2	no film		
7	**C_{16}Sulf**	1	patchy, poor adherence; much exposed wafer	220 nm + 120 nm roughness	amorphous
8	**C_{16}Sulf**	2	uniform, adherent (Figure 1c)	915 nm + 150 nm roughness	(001) anatase
9	**C_3Sulf**	1	nonuniform, poor adherence	180 nm + 150 nm roughness	amorphous
10	**C_3Sulf**	2	sparse, very patchy		
11	**PE**	1	patchy, poor adherence (Figure 1a); less exposed wafer than entry 7	270 nm + 95 nm roughness	amorphous
12	**PE**	2	uniform, adherent	915 nm + 150 nm roughness	(001) anatase
13	**PE**[d]	2	uniform, adherent (Figure 1d)	30 nm + 200 nm roughness	anatase

[a] Silicon wafers: cleaned by piranha solution, **P**; cleaned by UVOCS treatment, **U**; cleaned by initial solvent washes only, **C**; coated with a thioacetate-terminated SAM, **C_{16}TA**; coated with a sulfonate-terminated SAM, **C_{16}Sulf**; coated with short-chain sulfonate, **C_3Sulf**; coated with a sulfonate-capped polyelectrolyte multilayer, **PE**. [b] Method 1 after ref 3; method 2 after ref 7. [c] Determined by optical microscopy (up to 1000×). [d] Solution aged for 2 days at 50 °C and then filtered through a 0.25-μm filter, before TiO_2 deposition.

film was measured by a silicon surface barrier detector and analyzed by RUMP software for spectrum fitting to obtain the thickness and chemical composition of the films.

Substrate Preparation. Silicon wafers were cut into square pieces 1.5−2.0 cm on each edge. They were cleaned ultrasonically in hexane, dichloromethane, and ethanol. They were then dried under a filtered nitrogen flow. Subsequent cleaning and/or oxidation was done in one of two ways: (1) Substrates were dipped into "piranha solution" (a 30:70 mixture of 30% hydrogen peroxide (H_2O_2) and concentrated sulfuric acid kept at 80 °C) for 20 min. They were then washed by sonication in water. (2) Initially cleaned Si substrates were placed with their polished face up into the UVOCS cleaner for 10 min and used immediately upon removal.

Creating Thioacetate and/or Sulfonate-Bearing Silicon Substrates. *(a) Short-Chain Organic Sulfonate Film (C_3Sulf).* A piranha-treated silicon wafer was immersed into a solution of 3-mercaptopropyltrimethoxysilane (0.1 M) in toluene containing a few drops of glacial acetic acid. After 4 h at 65 °C, the sample was cleaned by sonication in dichloromethane and dried under a filtered nitrogen flow. The water contact angles of the surface were 75° (advancing) and 68° (receding). The measured thickness (ellipsometry) was 3.9 nm, considerably thicker than what would be expected for a simple monolayer film. Oxidation of the thiols to sulfonates was achieved by immersion into a saturated aqueous solution of oxone ($2KHSO_5 \cdot KHSO_4 \cdot K_2SO_4$, a monopersulfate oxidizing agent), for sufficient time that the substrate was fully wetted by water. The thickness of the oxidized surface was typically 3.1 nm, somewhat less than that of the initially deposited film. This may suggest that some loosely held material was released (due to electrostatic repulsion) from the initially deposited surface film.

(b) Long-Chain Organic Thioacetate SAM (C_{16}TA) and Sulfonate SAM (C_{16}Sulf). Deposition of 1-thioacetate-16-(trichlorosilyl)hexadecane from bicyclohexane solution onto a piranha-cleaned Si wafer used the procedure previously reported.[21,39,40] The C_{16}TA could be oxidized to a sulfonate-bearing SAM by immersion in a saturated aqueous solution of oxone for sufficient time that the substrate was fully wetted by water. The wetting properties of both the thioacetate and sulfonate SAM surfaces, as measured by contact angle goniometry, were identical to those previously reported.[39,41]

(c) Sulfonate-Capped Polyelectrolyte Multilayer (PE). The procedure of Chen and McCarthy[42] was used. A C_3Sulf surface was immersed in an acidic (pH = 2.2) solution of 0.02 M polyallylamine hydrochloride (PAA; M_w 50000−65000) and 1 M $MnCl_2$ for 20 min. It was then extensively rinsed with water. This ammonium-containing layer provided the template for the adsorption of polystyrene sulfonate (PSS; M_w 70000) by soaking it in an acidic (pH = 2.2) solution of PSS (0.02 M) and $MnCl_2$ (1 M) for 20 min. After being rinsed with water, the sample was once again treated with PAA and then with PSS to build alternately charged multilayer structures. Each multilayer consisted of 3 or 4 pairs of charged polyelectrolyte layers (6−8 layers). The final layer was always PSS.

Procedures for TiO_2 Deposition. In a procedure adapted from the work of Deki et al.[3−5,43] (method 1), variously prepared Si wafer substrates were immersed (standing on end) for 22 h at ambient temperature in a solution of 0.3 M H_3BO_3 and 0.1 M $(NH_4)_2TiF_6$. The initial pH of this solution was 3.88. When the variation reported by Koumoto et al.[7] (method 2) was used, the silicon wafer substrates were kept (standing on end) for 22 h at 50 °C in a solution of 0.15 M H_3BO_3 and 0.05 M $(NH_4)_2TiF_6$. The initial pH of this solution was adjusted to 2.88 by adding aqueous HCl. In one experiment, we used a modification of method 2, which involved aging the deposition solution at 50 °C for 2 days and then filtering it through a 0.25-μm filter, before immersing the substrate for 22 h.

All samples were cleaned ultrasonically in water and examined by optical and scanning electron microscopy, ellipsometry, XRD, and RBS. In experiments aimed at ascertaining the rate of film growth, deposition times were varied from a few hours up to ≈3 days.

Results

Table 1 summarizes the results of LPD depositions on substrates prepared using the procedures described above. In some cases, no TiO_2 film survived ultrasonic cleaning in water. In most cases a TiO_2 thin film was formed.

Silicon wafers without SAMs had been cleaned using either a conventional series of organic solvents, an UV ozone cleaner, or acidic piranha solution. The latter two more aggressive procedures are known to create a more hydrophilic surface oxide layer on the Si. Nevertheless, the mode of Si wafer activation (piranha or UVOCS) made no significant difference (Table 1, entries 2 and 3) in the deposition of the LPD TiO_2 film.

Method 1 gave patchy films on the sulfonate-bearing surfaces (Table 1, entries 7, 9, and 11; Figure 1a). On

(40) Collins, R. J.; Shin, H.; DeGuire, M. R.; Heuer, A. H.; Sukenik, C. N. *Appl. Phys. Lett.* **1996**, *69*, 860−862.
(41) Balachander, N.; Sukenik, C. N. *Langmuir* **1990**, *6*, 1621−1627.
(42) Chen, W.; McCarthy, T. J. *Macromolecules* **1997**, *30*, 78−86.
(43) Kishimoto, H.; Takahama, K.; Hashimoto, N.; Aoi, Y.; Deki, S. *J. Mater. Chem.* **1998**, *8*, 2019−2024.

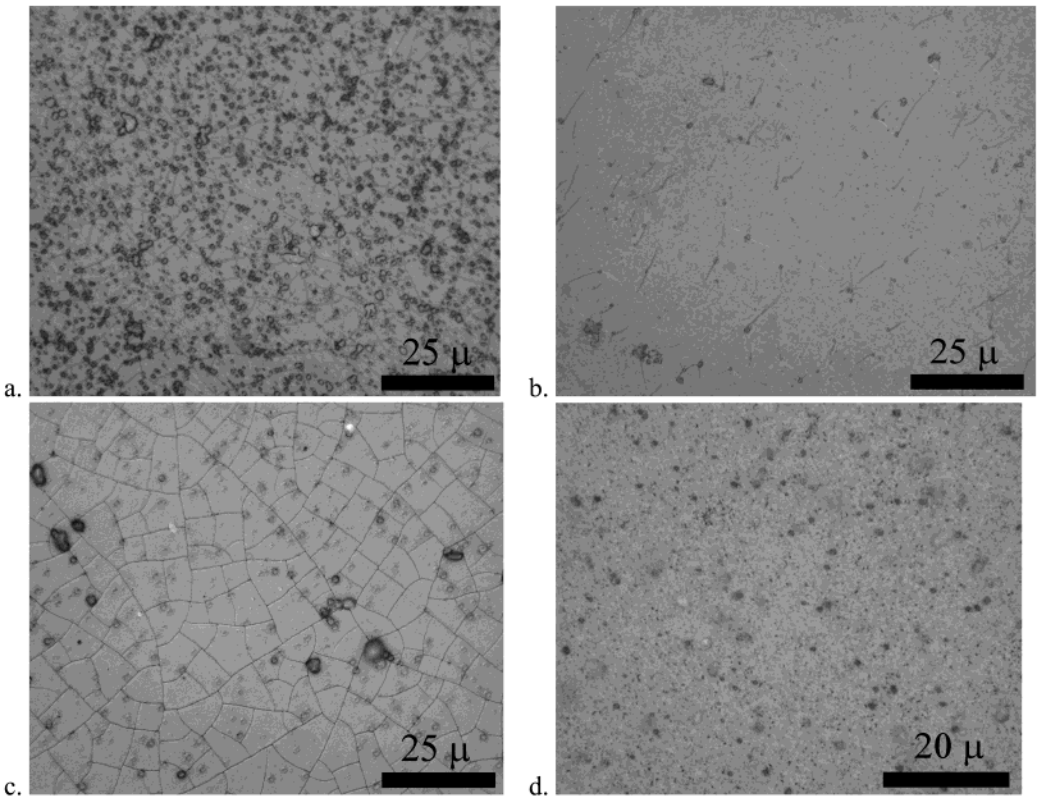

Figure 1. Optical micrographs of various prepared silicon surfaces, coated with LPD TiO_2 as described in the text: (a) Polyelectrolyte, method 1 (Table 1, entry 11). (b) Piranha-cleaned bare silicon, method 1 (Table 1, entry 2). (c) Long-chain sulfonated SAM, method 2 (Table 1, entry 8). (d) Polyelectrolyte with filtered solution (Table 1, entry 13).

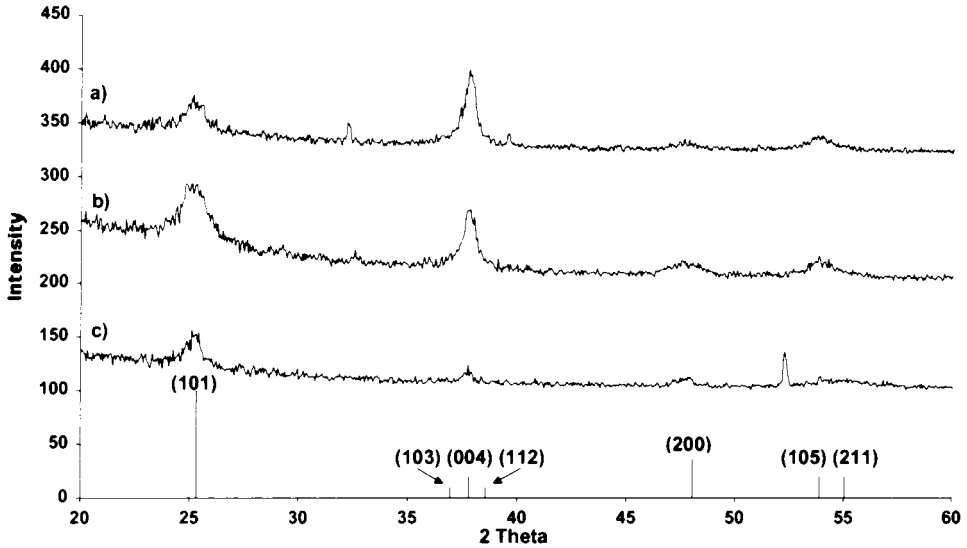

Figure 2. Grazing-incidence XRD spectra of LPD TiO_2 films deposited on different substrates via method 2: (a) C_{16}Sulf substrate (Table 1, entry 8). (b) PE substrate (Table 1, entry 12). (c) PE substrate, filtered solution (Table 1, entry 13). Bottom: Reference pattern for anatase (JCPDS 83-2243).

the silanol-bearing surfaces it gave uniform and continuous layers of TiO_2 (Table 1, entries 2−4; Figure 1b) ≈250−300 nm thick in 22 h. All films from method 1 were amorphous as determined by XRD.

Method 2, in contrast to method 1, gave badly incomplete films on the silanol-bearing surfaces and on C_3Sulf (Table 1, entries 1 and 10). However, it yielded full-coverage films 1-μm thick in 22 h on C_{16}Sulf (Figure 1c; Table 1, entry 8) and on the sulfonated polyelectrolyte (PE) surface (Table 1, entry 12). Unlike method 1, the films from method 2 were highly crystalline (anatase) with varying degrees of crystallographic orientation. For example, Figure 2a,b shows that the films obtained on PE and C_{16}Sulf surfaces exhibited significant orientation of the anatase *c*-axis perpendicular to the substrate, as evidenced by the enhanced intensity of the (004) peak relative to the (normally most intense) (101) peak. Oriented deposition of TiO_2 by LPD methods with[7] and without [6,8,9,44,45] prior functionalization of the

(44) Vigil, E.; Saadoun, L.; Ayllón, J. A.; Domènech, X.; Zumeta, I.; Rodríguez-Clemente, R. *Thin Solid Films* **2000**, *365*, 12−18.

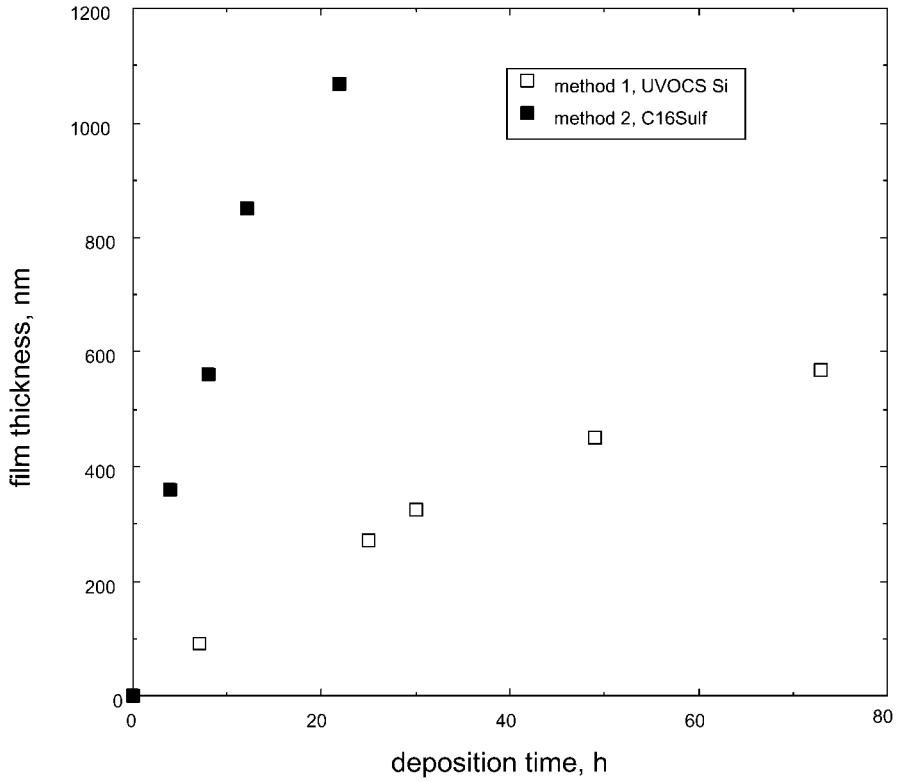

Figure 3. Dependence of TiO_2 film thickness (determined using ellipsometry) on deposition time for LPD method 1 on oxidized, hydrolyzed silicon (open symbols) and for LPD method 2 on C_{16}Sulf SAM on silicon (filled symbols).

substrate has been reported. In contrast, the film deposited from the filtered method-2 solution (Figure 2c; Table 1, entry 13) showed no preferred orientation. Application of the Scherrer formula[46] to estimate the crystal dimensions from the breadth of the (101) and (004) peaks indicates that the crystals were somewhat elongated: 5.4 nm in the [101] direction and 14 nm in the [001] direction for both of the oriented films. The crystals were somewhat larger but similarly elongated for the film from the filtered solution: 12 nm in the [101] direction and 18 nm in the [001] direction.

All solutions used in the present work initially exhibited visible turbidity. Solutions from method 1 tended to be less turbid than those from method 2, though they stayed turbid for 4−5 h (and then they settled), while those from method 2 were optically clear within 2 h. All but one of the films described here grew in unfiltered media, which may provide fine particles nucleated in the bulk of the solution. The one exception is shown in Table 1, entry 13, where the solution was clarified by filtration, leaving no visible turbidity. Figure 1d shows the resulting film, and Figure 2c shows its XRD pattern.

Figure 3 indicates the differences in growth rates attained by the two methods on their respective preferred substrates: bare Si substrates for method 1 (conditions analogous to Table 1, entry 3) and C_{16}Sulf for method 2 (conditions analogous to Table 1, entry 8). These thickness values were measured using ellipsometry. Thickness values (excluding roughness) obtained using RBS on these films were typically somewhat lower than those determined by ellipsometry and were 3−10% higher than the values obtained using ellipsometry if RBS roughness is included in the thickness values.

Independent of technique and substrate, films thicker than a few hundred nanometers exhibited cracks, attributed to stresses that result during drying of the film. For example, Figure 1c shows cracks in a method-2 film 1 μm thick, while Figure 1d shows an uncracked (but much thinner) method-2 film. (The film in Figure 1b does not appear to be cracked, but RBS detected exposed substrate; see below.) Figure 4 shows SEM micrographs of four of the method-1 films whose thicknesses are plotted in Figure 3. The 90 nm-thick film was uncracked (Figure 4a). In the 270-nm-thick film, the cracks are visible but closed (Figure 4b, note the absence of dark regions in the cracks). For thicker films (Figure 4c,d), the width of the cracks increased with increasing film thickness, and it was possible to quantify the area exposed (dark cracks) using image analysis. According to this measure, the 325-nm-thick film exposed 0.9% of the substrate (Figure 4c). This increased to 4.3 ± 0.2% in the 450-nm-thick film (not shown) and 5.7 ± 0.3% in the 570-nm-thick film (Figure 4d). The distance between cracks did not vary significantly with film thickness.

Interpretation of RBS Spectra. RBS provided an independent measure of film thickness and exposed substrate area. In addition it gave a semiquantitative indication of the roughness of the films. Figure 5 shows a representative RBS spectrum (Table 1, entry 2) from the present work.

The present specimens exhibited surface roughness on a lateral length scale that is small with respect to the beam size (1.5 × 1.5 mm^2). This leads to nonvertical slopes on the plateaus for each element in the affected layer(s). The fitting software models this spectral fea-

(45) Vigil, E.; Ayllón, J. A.; Peiró, A. M.; Rodriguez-Clemente, R.; Domènech, X.; Peral, J. *Langmuir* **2001**, *17*, 891−896.
(46) Cullity, B. D. *Elements of X-ray Diffraction*; 2nd ed.; Addison-Wesley Publishing Company, Inc.: Reading, MA, 1978.

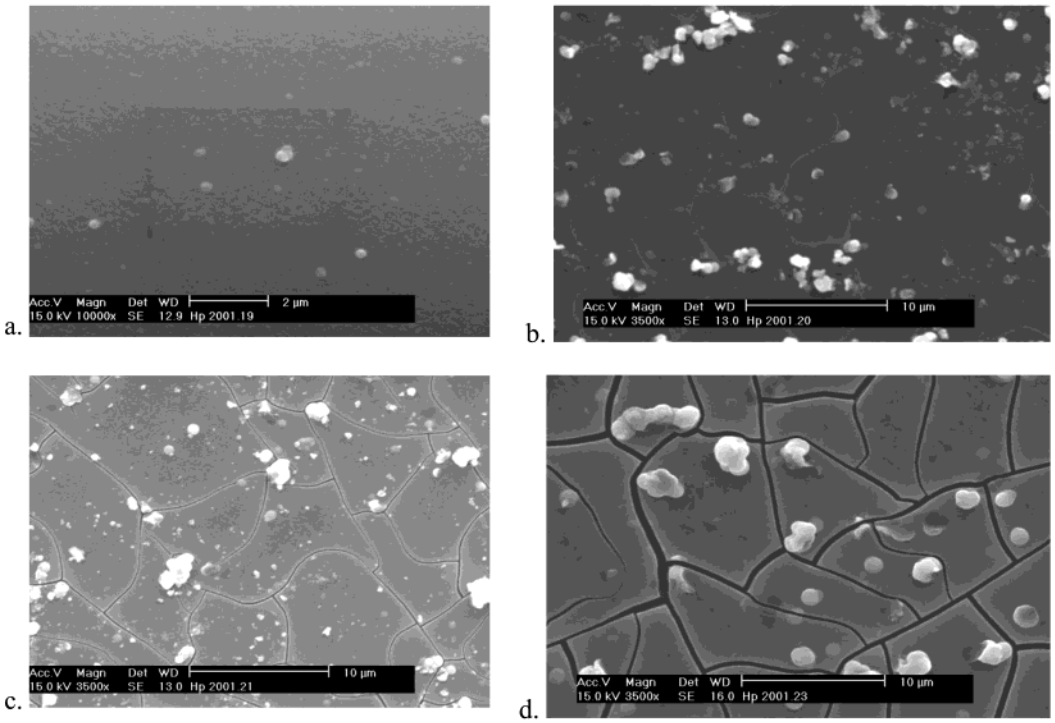

Figure 4. SEM micrographs of LPD TiO_2 films deposited using method 1 for various times: (a) 7 h, 90-nm thick, uncracked (bar = 2 μm); (b) 25 h, 270-nm thick (bar = 10 μm), cracks visible but closed; (c) 30 h, 325-nm thick, 0.9% area exposed by cracks (bar = 10 μm); (d) 73 h, 570-nm thick, 5.7% area exposed by cracks (bar = 10 μm).

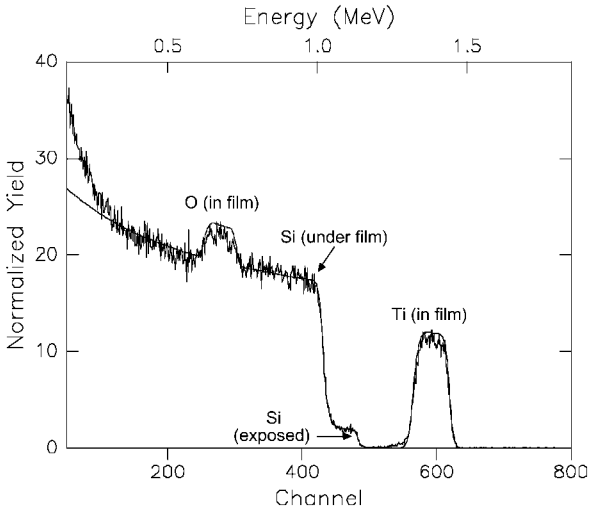

Figure 5. RBS spectrum of LPD TiO_2 film on Si (Table 1, entry 2) with fit. Roughness of the film is evident in the slightly nonvertical slopes of the plateaus, while exposed substrate adds a shoulder to the Si peak.

ture, providing an estimate of the surface roughness of the TiO_2 film (Table 1).

If any inner layer is exposed by gaps in the layer(s) above, the exposed portions (now effectively on the "top" of the specimen) will cause part of the corresponding plateau to be shifted upward in energy (to the right). Figure 5 illustrates this effect, with exposed Si from the substrate causing the appearance of a small but distinct shoulder on the silicon plateau, indicating the presence of cracks or bare regions of this film (Table 1, entry 2) that were not evident in optical microscopy (Figure 1b).

Discussion

Comparison of Present Results to Earlier Work. Deki and co-workers[3−5,43] obtained adherent TiO_2 films on glass, using solutions of 0.1−0.3 M H_3BO_3 and 0.05−0.15 M $(NH_4)_2TiF_6$. These films were largely amorphous as deposited, containing 37 vol % unoriented anatase.[43] In the present work, this method (method 1) yielded entirely amorphous films on oxidized Si, consistent with others' results on ITO-coated glass[47,48] and conductive SnO_2:F-coated glass.[49] A variation of LPD, using H_2TiF_6 and boric acid with a solution that had been presaturated with titania, also yielded amorphous films on Si.[50]

Koumoto et al.[7] used a lower pH (2.88 vs 3.88), used concentrations of $(NH_4)_2TiF_6$ and H_3BO_3 at the low end of the range studied by Deki, and raised the temperature of deposition from room temperature to 50 °C. Their work also differed from that of the Deki group in that their template was a Si wafer with surface silanols that had been installed by exposing a phenylsiloxane SAM to UV irradiation. The TiO_2 films obtained in this way showed good adherence to the silanols and poor adherence to the hydrophobic phenylsiloxane SAM. The films consisted of anatase with partial (001) orientation, as was observed in the present work on PE and C_{16}Sulf surfaces (Figure 2a,b). Vigil et al. also reported obtaining partially (001)-oriented anatase on ITO-coated glass by using microwave heating of an aqueous solution of 0.136 M HF, 0.068 M NH_4F, 0.034 M titanium isopropoxide, and 0.068 M H_3BO_3.[44,45] Shimizu et al.[6,8,9] reported depositing (001)-oriented anatase from aqueous solutions of TiF_4 at 40−70 °C on a variety of hydrophilic surfaces, including glass, polyethylene, polypropylene, poly(vinyl chloride), poly(ethylene terephthalate), phe-

(47) Wang, X. P.; Yu, Y.; Hu, X. F.; Gao, L. *Thin Solid Films* **2000**, *371*, 148−152.
(48) Wang, X. P.; Yu, Y.; Gao, L.; Hu, X. F. *J. Inorg. Mater.* **2000**, *15*, 573−576.
(49) Richardson, T. J.; Rubin, M. D. *Electrochim. Acta* **2001**, *46*, 2119−2123.
(50) Lee, M.-K.; Lei, B.-H. *Jpn. J. Appl. Phys.* **2000**, *39*, L101−L103.

nol resin, cotton fiber, and filter paper. The question of why these films were oriented and crystalline, while the films from the Deki route were not, is addressed later in the text.

Deki's group[3,5] reported obtaining films up to 800 nm thick, with little or no slowing in the growth rate for times up to 80 h. Their growth rates (either reported directly[3] or as-extracted from their quartz crystal microbalance data, corrected to their SEM observations of film thickness[5]) ranged from 5 to 25 nm h^{-1}, depending on the composition of the solution. In the present work, the maximum film thickness obtained via method 1 was 570 nm in 73 h, with an initial growth rate of 13 nm h^{-1} in the first 7 h (Figure 3), dropping to 5 nm h^{-1} after 50 h. Method 2 gave a significantly higher growth rate of 70 nm h^{-1} for the first 12 h (Figure 3) in the present work. (The original paper[7] describing method 2 does not report growth rates.)

Under different deposition conditions, Xiao et al. obtained LPD TiO_2 films on C_3Sulf [24−26] surfaces, although the absence of receding contact angles and thickness data for their organic surfaces prevents a more detailed comparison to the present work. Also under different deposition conditions, Fendler and coworkers obtained TiO_2 films on polyelectrolyte surfaces.[36,37] These reports further illustrate the interdependence of solution and substrate chemistries in producing a film: the optimum solution for one surface may not be optimum for another surface and vice versa. To underscore this point, it is worth noting that the solutions used in all of these cited studies grew films more slowly than those in the present work.

Effect of Substrates. For both LPD methods used in the present work, a thin hydrophobic coating (the thioacetate-terminated SAM) prevented formation of an adherent film (Table 1, entries 5 and 6). These results are consistent with Koumoto's report[7] that LPD TiO_2 films did not adhere to phenylsiloxane layers. The effect is not limited to LPD, occurring when titania films form via simple hydrolysis of $TiCl_4$ using thioacetate-[40] or methyl-[21] terminated SAMs and via hydrolysis of titanium lactate in the presence of a vinyl-terminated SAM.[23] Nor is the effect limited to aqueous deposition media: Masuda et al.[28] recently reported that hydrolysis of a solution of titanium dichloride diethoxide in toluene did not yield a film on octadecyltrichlorosilane SAMs.

The two LPD variations used here showed an interesting distinction with regard to specificity of deposition on certain surfaces. That is, while method 2 worked well on sulfonate-rich surfaces (Table 1, entries 8, 12, and 13), method 1 did not (entries 7, 9, and 11); and while method 1 worked well on Si/SiO_2 surfaces (entries 2, 3, and 4), method 2 did not (entry 1).

The specificity of deposition between methods and surfaces observed in the present work may be accounted for qualitatively by the pH of methods 1 and 2 relative to the isoelectric points of TiO_2 and SiO_2. In both methods, the pH (3.88 for method 1, 2.88 for method 2) is below the isoelectric point of TiO_2 (reported values of which range among 5.6,[51] 5.9,[52] and 6.2[53]). TiO_2 forming under these conditions will therefore have a positive surface charge density and would be expected to experience a significant electrostatic attraction to surfaces with negative surface charge density. Reported values of the isoelectric point of SiO_2 (i.e., the oxide surface of Si) range from 1.8[54] to 2.7.[55] That is, the surface of the oxidized silicon wafer will be negatively charged at the pH (≈4) of method 1 and less so at the pH (≈3) of method 2. For deposition on "bare" SiO_2, the better coverage and quality of films obtained using method 1 thus may result from the increased electrostatic attraction of TiO_2 to SiO_2 at the higher pH relative to that of method 2.

The excellent adherence of films from method 2 to uniformly functionalized sulfonate-bearing surfaces is likewise consistent with this reasoning, as the sulfonate surface is expected to be much more negatively charged than bare Si, even under these acidic conditions. The ability of sulfonate groups to enhance the formation of TiO_2 films is well known; it has been reported for hydrolysis of both $TiCl_4$[21,40] and titanium lactate[23] in strongly acidic solutions.

In other studies of the effect of various SAM terminations, Nagtegaal et al.[15,16] used thiol-anchored SAMs on gold as surfaces for deposition of iron oxyhydroxide films. Films were observed to form on sulfonate SAMs, on gold, and on uncoated glass substrates, but not on alcohol-, methyl-, carboxylate-, phosphonate-, or (amine hydrochloride)-terminated surfaces. They attributed this specificity to the ability of the sulfonate group, alone among the functionalities studied, to deprotonate even in acidic environments, binding positively charged iron ions or complexes from the solution.

Aizenberg et al.[34] studied the formation of calcite crystals from aqueous solution on thiol-anchored SAMs on gold and silver. Compared to the bare metal surfaces, calcite nucleates preferentially on hydroxyl and phosphonate SAMs and especially on carboxylate and sulfonate SAMs. Methyl-terminated SAMs suppress nucleation, and trimethylammonium salt-terminated SAMs prevent nucleation. While calcite nucleates on a wider variety of surface functionalities than does iron oxyhydroxide,[15,16] the most striking difference is that each combination of underlying metal and preferred surface termination nucleates a distinct orientation of calcite crystals, with specificity for the calcite polymorph at or near 100% and high degrees of crystallographic orientation (exceeding 70% for carboxylate and hydroxyl SAMs).[34] (The question of oriented films in the present work is addressed below.)

In light of the preceding discussion, the inability to form good films on sulfonated surfaces via method 1 here is unexpected, as the same reasoning based on electrostatic attractions between film and substrate should apply to both methods with regard to sulfonated surfaces. This result may be related to the fact that, at the higher pH (≈4) of method 1, the positive surface charge density of TiO_2 will be smaller than that at the pH (≈3) of method 2. (In fact, one source[55] gives the

(51) Larson, I.; Drummond, C. J.; Chan, D. Y. C.; Grieser, F. *J. Am. Chem. Soc.* **1993**, *115*, 11885.
(52) Wiese, G. R.; Healy, T. W. *J. Colloid Interface Sci.* **1975**, *51*, 427−433.
(53) Yotsumoto, H.; Yoon, R. H. *J. Colloid Interface Sci.* **1993**, *157*, 426.
(54) Veeramasuneni, S.; Yalamanchili, M. R.; Miller, J. D. *Colloids Surf. A* **1998**, *31*, 77.
(55) Subramaniam, K.; Yiacoumi, S.; Tsouris, C. *Colloids Surf. A* **2000**, *177*, 133−146.

isoelectric point of TiO_2 as 4−5, which would suggest that the positive surface potential on TiO_2 would be very small at a pH of 3.88.) The negative surface charge of the strongly deprotonated sulfonate surface, in contrast, should be large and relatively insensitive to pH.

The first report of method 2 described adherent crystalline TiO_2 films being formed on the silanol layer that is left behind from the photocleavage of a siloxane-anchored SAM from Si.[7] A similar effect was reported when the deposition medium was a nonaqueous solution of titanium dichloride diethoxide in toluene.[28] This contrasts with the present work in which method 2 did not yield adherent films on UVOCS- or piranha-cleaned Si (Table 1, entry 1a,b). Nominally, all three types of silicon surfaces are terminated with silanol (Si−O−H) groups, so the explanation of the divergent results is not clear. If the films formed via heterogeneous nucleation of titania particles on the surface, the results of Koumoto et al. indicate that the silanol group left behind on Si after photocleavage of a silane-anchored SAM is clearly more reactive toward formation of Si−O−Ti bonds than are the silanol groups on UVOCS- or piranha-cleaned Si. If the films formed via attachment of pre-existing titania particles, there could additionally be some differences in either the ionic double layer or the effective local pH of the two types of silanol surface that might account for the difference in adherence of TiO_2 particles.

Effect of Solution on Growth Rate. The growth rate obtained in the present work using method 2 (70 nm h^{-1}) was dramatically higher than that of method 1 (initially 12 nm h^{-1}). Substrate effects would not be expected to account for such a difference; once the first few nanometers of film have formed, the influence of the substrate on film growth is at most indirect. Rather, solution chemistry and temperature will determine the degree of supersaturation of the system, which will have a strong influence on the ability of the liquid medium to supply material to the growing film. Increasing supersaturation should increase the rates of nucleation and growth of solid, which may lead to increased growth rates of the film.

In aqueous hydrolyzing systems, supersaturation of a solution can be increased by raising the temperature, raising the concentration of the metal, or (when starting from the acidic side of the solution−precipitation equilibrium, as in the solutions used here) by raising the pH. Here, the higher temperature of method 2 over method 1 (50 °C vs ≈25 °C) was apparently the dominant factor of the three; the solution in method 2 became turbid and settled in just 1.5−2 h (vs 4−5 h in method 1) despite its lower pH (3 vs 4) and slightly lower metal concentration. This implies that the kinetics of crystallization were more rapid in method 2, contributing to the observed higher growth rate.

Excessively high supersaturation typically leads to heavy bulk precipitation. In some cases this can eliminate the supersaturation in the deposition medium, stopping film growth. On the other hand, if the solution remains supersaturated after bulk precipitation occurs (as was apparently the case with both methods used here), growth can proceed via heterogeneous nucleation, attachment of (nano)particles, or both.[1] Growth via attachment of particles is usually associated with high growth rates, but also high roughness and reduced crystallographic orientation. Method 2 here avoided this compromise, yielding a high growth rate as well as partial crystallographic orientation and the smoothest surfaces (as a percentage of film thickness) observed in this work. Optimizing the film growth rate usually involves balancing factors that increase supersaturation with those that favor a more controlled formation of solid at or near the film−solution interface.

Effect of Substrate and Solution on Crystallinity and Orientation of Films. From the literature as well as the present study, it is clear that the crystallinity of LPD titania films depends in part on solution parameters. Solutions with both lower titanium concentrations and ligands such as F^-, SO_4^{2-}, and urea (H_2NCONH_2) that coordinate strongly to titanium favor the formation of crystalline films.[6−9,44] In most of these cases, the crystalline phase is anatase; Yamabi and Imai[10] report that films of the rutile polymorph of titania can be obtained from solutions at relatively low degrees of supersaturation. Amorphous films have been reported from solutions with higher titanium concentrations or less strongly complexing ligands for titanium.[3−5,43,47−50]

Once a polycrystalline film is nucleated, its final crystallographic orientation may depend on a variety of factors. As Rodriguez-Navarro and Garcia-Ruiz have pointed out,[56] some of these factors are substrate-independent; that is, oriented films do not necessarily imply that oriented nucleation has occurred. For example, if the crystal growth rates are anisotropic, the film will tend to exhibit so-called "fiber texture," that is, with either a fast axis predominantly perpendicular to the film or a slow axis oriented parallel to the film. Growth rate anisotropy can in turn be strongly influenced by the solution composition, for example, by preferential adsorption of ionic or polymeric species from the solution onto certain crystallographic faces, slowing growth normal to these faces.[57,58] The elongated growth habit of the crystals in the present films (inferred from the XRD measurements, with particle sizes parallel to [001] being 1.5−2.6 times larger than the size parallel to [101], consistent with SEM and TEM observations on anatase films by Yamabe and Imai[57]) indicates that such growth anisotropy exists in anatase.

In addition, specific substrate−crystal relationships can result in high degrees of crystallographic texturing, as shown, for example, by Aizenberg et al. for calcite on various SAMs.[34] Therefore, a detailed analysis of both growth anisotropy and substrate−film interfacial structure would be necessary to determine the cause of orientation in any specific case.

With this in mind, we suggest one substrate-related factor that may have contributed to the observed (001) orientation of the anatase films obtained via method 2 in the present work. Of the low-index planes of anatase (i.e., planes with high atomic density, which would be likely preferred surfaces for film growth), only the planes perpendicular to the *c*-axis are polar (i.e., are planes that contain either all cations or all anions). This polarity results from a slight offset of oxygen atoms

(56) Rodriguez-Navarro, A.; Garcia-Ruiz, J. M. *Eur. J. Mineral.* **2000**, *12*, 609−614.
(57) Yamabi, S.; Imai, H. *Chem. Mater.* **2002**, *14*, 609−614.
(58) Grohe, B.; Miehe, G.; Wegner, G. *J. Mater. Res.* **2001**, *16*, 1901−1910.

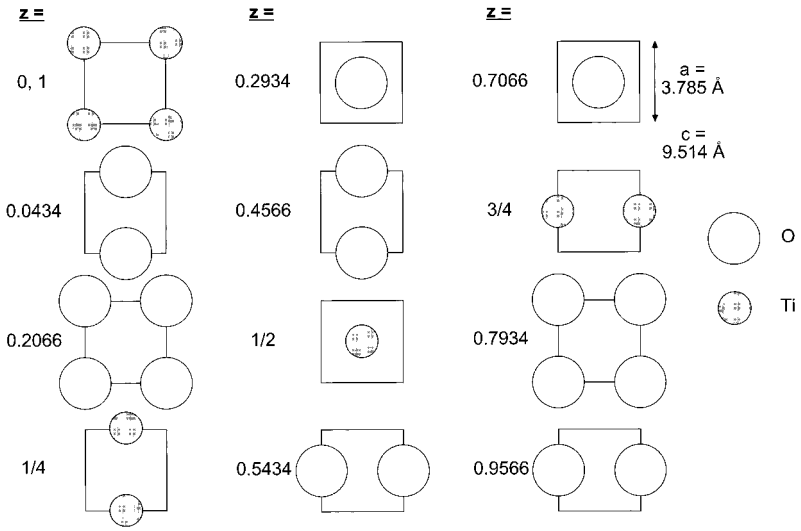

Figure 6. Stacking sequence of planes along the (001) direction of anatase (after ref 60).

above and below the (00*l*)-type planes that contain the Ti atoms[59,60] (Figure 6). A substrate with a high concentration of surface charges, such as the negatively charged PE and C_{16}Sulf surfaces in the present experiments, would therefore present a favorable nucleation site for *c*-axis-oriented anatase (in this case, starting with a cation layer). The more planar of these two surfaces on the atomic scale, C_{16}Sulf, would be expected to, and did, give the higher degree of *c*-axis orientation, as evidenced by the higher (004) peak relative to the normally strongest (101) peak (Figure 2). Though the polyelectrolyte layer completely covers the silicon wafer, it is rougher and more disorganized than a well-formed SAM.

The poor film reported from method 2 on C_3Sulf (entry 10) is likely the result of the known tendency for short-chain surface modification agents to provide nonuniform surface coverage with a mixture of layer thicknesses and chain orientations. Furthermore, the trichlorosilane group used to anchor the C_{16} SAM is better suited for ordered monolayer formation than is the trialkoxysilane group used herein. These effects are supported by the relatively large hysteresis in contact angle and large thickness reported in the preparation of the C_3 surfaces (see Experimental Procedure). The surface, although negatively charged, presumably lacked sufficient concentration and regularity of surface charge to make an effective template for nucleation of a close-packed oxide crystal such as anatase. This reasoning would apply even more so to the bare Si surface (entries 1a,b). On the other hand, if the solution chemistry was such as to produce an amorphous solid, there would be no particular preference for polar over nonpolar substrates (as in method 1 here).

We note that entry 13 in Table 1, deposited via method 2 but with a solution that had been aged and filtered to remove bulk precipitates, nevertheless appears to have grown primarily by particle attachment: its diffraction pattern is virtually identical to that of randomly oriented anatase (Figure 2c), and it is the roughest film (as a percentage of total film thickness) produced in this work. Undoubtedly the aging reduced the solution's supersaturation, which would have slowed heterogeneous nucleation and growth; this film was much thinner than its unaged, unfiltered counterparts (Table 1, entries 8 and 12). Nanoparticles, small and numerous enough to initiate film growth, may have escaped the filtering process and formed the film along with additional particles nucleated later in the bulk solution.

It is interesting to compare the preceding results to systems based on simple hydrolysis. The hydrolysis of TiF_4 in solutions of pH 1.0−3.1 on a wide range of substrates is reported[6,8,9] to lead to the growth of unoriented anatase. The only substrate dependence reported is that hydrophilic substrates give adherent films and hydrophobic substrates do not. The hydrolysis of $TiCl_4$[21,40] in strong acid at 80 °C yields crystalline anatase on C_{16}Sulf with no preferred orientation. Titanium lactate hydrolysis in aqueous acid solution also produces unoriented crystalline anatase on C_{16}Sulf but amorphous titania on sulfonated polycarbonate.[23] The presence of charged surfaces, such as ordered sulfonate SAMs, thus may favor the formation of oriented anatase films but is not a sufficient condition.

Conclusions

To allow for systematic changes in substrate structure, all work reported herein was done on variously treated Si wafers. This allowed us to identify fundamental differences among solution deposition conditions and to assess how they are affected by changes in surface charge and/or functionality. Moderately hydrophobic surfaces effectively prevent TiO_2 deposition. Proper choice of solution conditions (method 1) allowed hydrophilic silicon wafer surfaces to be coated with adherent, conformal films of amorphous TiO_2. By contrast, method 2 gave poorly adherent, patchy films on these clean silicon surfaces. We ascribe this difference to insufficient electrostatic attraction between substrate and film at method 2's lower pH.

On the other hand, surfaces bearing sulfonate functionality (from a C_{16}-sulfonate SAM or complete cover-

(59) Wyckoff, R. W. G. *Crystal Structures*; 2nd ed.; Interscience: New York, 1963; Vol. 1.
(60) Wells, A. F. *Structural Inorganic Chemistry*, 5th ed.; University Press: Oxford, 1975.

age by sulfonated polyelectrolyte) promoted film deposition using method 2. This result is understandable in terms of the strong negative surface charge density provided by such sulfonated surfaces even under acidic conditions, and the smaller but positive surface charge of TiO_2 in moderate to strong acids. In contrast, the sulfonated surfaces gave no film formation under method 1 conditions. This, like the negative result of method 2 with bare Si, may be due to insufficient electrostatic attraction between the film and the substrate at the pH of the method.

The lower-pH conditions (method 2) are also sensitive to the kind of sulfonated surface. A surface that has been functionalized with a short-chain (C_3) sulfonate does not present a well-organized monolayer, but is rather a heterogeneous surface with some sulfonate groups exposed. Such a surface is not nearly as effective in promoting film deposition as a C_{16}-sulfonate SAM with its dense, uniform array of sulfonates. On the other hand, the sulfonate-bearing surface presented by sulfonated polyelectrolyte is effective in this regard. The polyelectrolyte surface presents a high concentration of sulfonate groups, even though they are likely to be at least partially intertwined within the layers of polymer.

We also find that the higher temperature of method 2 promotes more rapid film growth. Interestingly, this does not undermine the (001)-oriented crystallization arising from the interaction of the anatase with the highly anionic sulfonated surfaces. This oriented crystal growth, which is observed on both the C_{16} SAM sulfonate and on the PE-sulfonate, is likely initiated by the nucleation of the cationic (001) plane of anatase on the deprotonated sulfonate surfaces. We note that the Ti−Ti spacing in the (001) plane of anatase, 0.379 nm, is ≈10% smaller than the interchain spacing, 0.425 nm, suggested for an ordered SAM made from a trichlorosilane surfactant.

Acknowledgment. The authors gratefully acknowledge support from the Israeli Ministry of Science Tashtiyot Program, from the Germany-Israel Program (DIP) of the German DLR, and from the U.S. National Science Foundation (Grant DMR 9803851). The authors thank Prof. Arthur Heuer (CWRU) and Dr. Thomas Niesen (Siemens & Shell Solar, Munich) for critical reading of the manuscript and constructive comments.

CM010776E